Developing an IGS Time Scale

Ken Senior, Paul Koppang, Demetrios Matsakis, and Jim Ray

Abstract— **Currently, the International GPS Service (IGS) provides a set of clock products for both satellites and tracking receivers, tabulated at 5-minute intervals. These products provide users with sufficient information to determine consistent coordinates and clock values for an isolated GPS receiver with a precision at roughly the 5-cm level. However, because the underlying time scale for the IGS combined clocks is based on a linear alignment to broadcast GPS time for each day separately, the day-to-day stability of this reference is poor. We show the results of a new filter package written to automate the production of an integrated IGS frequency scale loosely steered to GPS time and to which the IGS clock products will soon be referenced.**

Keywords— **GPS, IGS, Time Scale, Frequency Scale, Control, Carrier-Phase Time Transfer**

I. Introduction

ON November 5, 2000 (GPS week 1087), a new set of IGS clock products, consisting of combined estimates of GPS satellite clocks and a subnetwork of IGS tracking stations submitted by several IGS analysis centers, became official [1]. TABLE I summarizes the current mix of clocks contained in the IGS combined clock subnetwork. Tabulated at 5-minute intervals, use of these estimates together with IGS orbits instead of broadcast information allows for Precise Point Positioning (PPP) results [2] at the 5-cm level for individual, isolated GPS receivers. In addition, feedback is provided to station operators on the performance of local clocks. However, each clock estimate in the IGS combined clock product is referenced to a daily linear alignment to GPS time, herein referred to as GPST, resulting in large offsets in time and frequency between days (see Figure 1). The purpose of this paper is to introduce a near-real time system recently implemented for creating a new more stable reference for these clock estimates consisting of a weighted ensemble of the clocks in the IGS combined clock product.

TABLE I
Current (January, 2001) mix of clocks contained in the IGS combined clock product.

No.	Type
29	Hydrogen Maser
14	Cesium
8	Rubidium
23	Crystal
6	GPS Block IIR Rubidium
17	GPS Block II/IIA Cesium
6	GPS Block IIA Rubidium

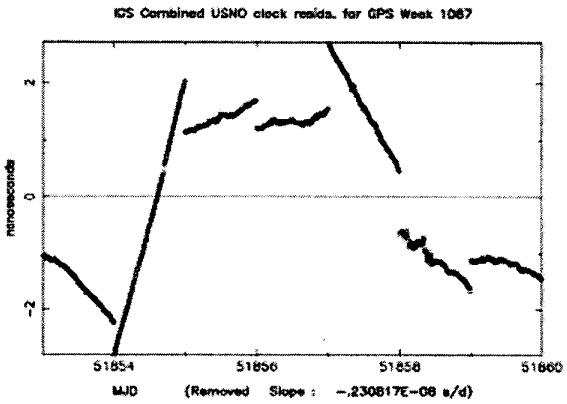

Fig. 1. IGS combined clock estimate of a steered Sigma Tau hydrogen maser located at USNO in Washington, D.C.. The estimate is referenced to a daily linear alignment to GPS time (GPST). The plot shows the large day-to-day offsets in phase and frequency resulting from the GPST alignment strategy. This plot was obtained from http://maia.usno.navy.mil/gpstclocks/finals.

II. Filter and Integrated Frequency Scale Algorithm

Most IGS station receiver systems' internal clocks may reset to an arbitrarily large value (e.g. from power cycling of the system), resulting in potentially large phase jumps in the clock estimates. Also, standard reductions of GPS carrier-phase data often result in discontinuities of clock estimates at processing boundaries of up to a nanosecond (e.g. a result of averaging pseudorange data over daily arcs). Moreover, the overall phase bias between the IGS receivers and UTC contributor clocks is unknown (i.e. IGS receiver systems are uncalibrated). Because of these considerations and because frequency is the fundamental quantity in atomic clocks (c.f. [3]), the algorithm for filtering the IGS combined clock estimates into a time scale was formulated as an integrated frequency scale. That is, phase estimates for each clock are used to form fractional frequency measurements (over 5-minute intervals) of each clock. Outliers (i.e. phase jumps) are removed and discrete jumps in frequency are detected (see details in section E). A simple linear model (quadratic in phase) is fit to the frequency measurements to detrend each clock against the frequency scale, which is formed on-the-fly in the filter using a standard weighting scheme (section F). After iterating with respect to the weights, the time scale is formed by taking the final weighted average of the detrended fractional fre-

Authors are with the U.S. Naval Observatory, Washington, D.C., U.S.A., E-mail: ksenior@usno.navy.mil, koppang.paul@usno.navy.mil, matsakis.demetrios@usno.navy.mil, jimr@maia.usno.navy.mil .

U.S. Government work not protected by U.S. copyright

quency estimates of each clock and integrating back into a time series. This time scale is then steered to GPST with a slow time constant. That is, the new time scale is loosely steered to GPS time, resulting in a reference which is more stable than GPST in the short term, but maintaining a link to GPS time in the longer term. Each IGS clock is then re-referenced to the new steered time scale.

A. Clock Model

We estimate the frequency (or rate) and frequency aging (or drift) of each clock using a two-state vector polynomial $\vec{p}(t)$ driven by white noise processes. We denote this in the usual state-space formulation (discrete-time) as (cf. [4], and [5])

$$\vec{p}(t_{i+1}) = \varphi(\tau)\vec{p}(t_i) + \vec{e}(t_i), \quad \varphi(\tau) = \begin{bmatrix} 1 & \tau \\ 0 & 1 \end{bmatrix}, \quad (1)$$

$t_{i+1} = t_i + \tau$, where the first and second components of $\vec{p}$ are rate and drift respectively, and where the two components of $\vec{e}$ are independent white noise processes.

Given frequency measurements $Y(t)$ for a clock, we specify the measurement model as

$$Y(t) = \mathbf{h}\vec{p}(t) + n(t), \quad \mathbf{h} = \begin{bmatrix} 1 & 0 \end{bmatrix} \quad (2)$$

where n is a scalar white noise sequence which is assumed independent of the process noise $\vec{e}$. For approximate (i.e. for small τ) modelling of Random Walk FM, and Random Run FM one would require that the covariance $\mathbf{q}$ for $\vec{e}$ be specified as (cf. [3], [6], [7], [8], and [9]),

$$\mathbf{q} \stackrel{\text{def}}{=} E[\vec{e}\,\vec{e}^{\,T}] = \begin{bmatrix} a_{-1}\tau + a_{-2}\frac{\tau^3}{3} & a_{-2}\frac{\tau^2}{2} \\ a_{-2}\frac{\tau^2}{2} & a_{-2}\tau \end{bmatrix}, \quad (3)$$

and for approximate modelling of White FM the covariance r for n be given as,

$$r \stackrel{\text{def}}{=} E\left[n^2\right] = \frac{a_0}{\tau},$$

where a_0, a_{-1}, and a_{-2} are the noise spectral densitities of White FM, Random Walk FM, and Random Run FM respectively which may be experimentally determined by analyzing Allan variances (or perhaps Hadamard variances which are insensitive to drift) for each clock.

B. System of clocks and the frequency scale equation

Individual clocks will be denoted by parenthetic superscripting. The scale to which each clock is referenced will either be clear from the context or will be specified in the subscript. The state-space formulation (1)-(2) is generalized to a system of N clocks by setting (cf. [10]):

$$\vec{P}(t_{i+1}) = \mathbf{\Phi}(\tau)\vec{P}(t_i) + \vec{\varepsilon}(t_i) \quad (4)$$

$$\vec{Z}(t_{i+1}) = \mathbf{H}\vec{P}(t_{i+1}) + \vec{\eta}(t_{i+1}) \quad (5)$$

where

$$\vec{P} = \begin{bmatrix} \vec{p}^{(1)} \\ \vec{p}^{(2)} \\ \vdots \\ \vec{p}^{(N)} \end{bmatrix}, \quad \mathbf{H} = \begin{bmatrix} \mathbf{h} & & & \\ & \mathbf{h} & & \\ & & \ddots & \\ & & & \mathbf{h} \end{bmatrix},$$

$$\mathbf{\Phi} = \begin{bmatrix} \varphi & & & \\ & \varphi & & \\ & & \ddots & \\ & & & \varphi \end{bmatrix},$$

$$\vec{\varepsilon} = \begin{bmatrix} \vec{e}^{(1)} \\ \vdots \\ \vec{e}^{(N)} \end{bmatrix}, \quad \vec{\eta} = \begin{bmatrix} n^{(1)} \\ n^{(2)} \\ \vdots \\ n^{(N)} \end{bmatrix},$$

and where the corresponding covariances for $\vec{\varepsilon}$ and $\vec{\eta}$ may be written respectively as,

$$\mathbf{Q} = \begin{bmatrix} \mathbf{q}^{(1)} & & & \\ & \mathbf{q}^{(2)} & & \\ & & \ddots & \\ & & & \mathbf{q}^{(N)} \end{bmatrix}, \text{ and}$$

$$\mathbf{R} = \begin{bmatrix} r^{(1)} & & & \\ & r^{(2)} & & \\ & & \ddots & \\ & & & r^{(N)} \end{bmatrix}.$$

The data vector $\vec{Z}$ is specifed in the following way. Labelling the IGS combined clock phase estimate (referenced to GPST) for each clock j as $X^{(j)}_{\text{GPST}}$, we form fractional frequency measurements $Y^{(j)}_{\text{GPST}}$ over each $\tau = 5$ minute interval (time-tagged at the end of each interval) according to

$$Y^{(j)}_{\text{GPST}}(t_{i+1}) = \frac{X^{(j)}_{\text{GPST}}(t_{i+1}) - X^{(j)}_{\text{GPST}}(t_i)}{\tau}.$$

Each component Z_j of the data vector $\vec{Z}$ in (5) is set to

$$Z_j(t_{i+1}) \stackrel{\text{def}}{=} Y^{(j)}_{\text{GPST}}(t_{i+1}) - \sum_{k=1}^{N} w_k(t_{i+1}) \left(Y^{(k)}_{\text{GPST}}(t_{i+1}) - \left(\varphi \vec{p}^{\,(k)}(t_i) \right)_1 \right) \quad (6)$$

where the weights w_k for the clocks (section F) are such that

$$\sum_k w_k(t) = 1 \quad (7)$$

for each t.

The standard frequency scale equation (6) detrends the data for each clock *with respect to the new scale* at $t = t_{i+1}$ using current estimates of its rate and drift (as propagated from t_i to t_{i+1} by φ). This is particularly useful in this application since at any 5-minute epoch, up to 1/10 of the

clocks transition in or out of the filter because of data outages and to a lesser extent because of data editing. Equation (6) ensures that as clocks move in and out, the scale will be minimally affected.

In support of the continuing move of the IGS to real-time production of its products, a standard Kalman filter is employed to solve (4)-(5), allowing one to process data sequentially in batches (currently, 1-day batches) and to model the noise processes mentioned earlier. Moreover, subject to the underlying assumptions, the Kalman approach yields optimal state estimates and can accept data at arbitrary τ intervals ([11] and [9]). Currently, two iterations of the filter are performed in order to refine the weights. The filter accomodates the changing size of the state vector and covariance matrix as the number of clocks varies by updating only those subcomponents or submatrices of the state and covariance for which data are available.

C. Filter Output

Aside from individual estimates of the rate and drift of each clock relative to the new frequency scale, the primary output of the Kalman filter implementation of (4)-(5) is a single series,

$$\sum_{k=1}^{N} w_k(t) \left(Y^{(k)}_{\mathrm{GPST}}(t) - \overrightarrow{p}^{(k)}_1(t) \right) \stackrel{\mathrm{def}}{=} Y^{\mathrm{IGST}}_{\mathrm{GPST}}(t) \qquad (8)$$

of the new frequency scale relative to the original scale GPST. Note that it is unnecessary to detrend each clock with respect to its drift estimate $\overrightarrow{p}^{(k)}_2(t)$ since φ in (1) ensures that drift is already accounted for in $\overrightarrow{p}^{(k)}_1(t)$. Integrating (8) this frequency series yields its corresponding times series which we label as $X^{\mathrm{IGST}}_{\mathrm{GPST}}(t)$, where we have labelled the new time scale as IGST. Once this series is obtained, we may re-reference all of the original clock estimates in the IGS combined clock product by simple subtraction,

$$X^{(j)}_{\mathrm{IGST}}(t) = X^{(j)}_{\mathrm{GPST}}(t) - X^{\mathrm{IGST}}_{\mathrm{GPST}}(t), \qquad (9)$$

so that relative clock-to-clock measures—and hence the use of the re-referenced clocks in positioning applications—are unaffected. However, before performing this re-referencing, we loosely steer the time scale to GPS time (see section G below).

D. $\mathbf{Q}$ and $\mathbf{R}$

Though the package has been written to include modelling of the noise processes mentioned above, more work must be done to better determine estimates of the parameters necessary to appropriately model all of these noise processes. Currently, only a minimal amount of Random Walk FM and Random Run FM noise is injected into the filter for each clock in order to maintain stability of the filter (cf. [7], p. 261). Future enhancements will consider improved estimates of the parameters a_{-1} and a_{-2} in (3) for these noise types.

Also, the White FM model has been modified to impose better data weighting in the filter based on formal errors for each clock which are included in the IGS combined clock product. That is, in addition to estimates of the phase $X^{(j)}_{\mathrm{GPST}}(t)$ of each clock, the IGS combined clock product also provides formal errors $\sigma^2_{X^{(j)}}(t)$ for each clock which are a measure of the agreement among the analysis center estimates. We use these formal errors as measurement error input to the frequency scale filter by setting,

$$\begin{aligned} r^{(j)}(t_{i+1}) &= \frac{\sigma^2_{X_j}(t_{i+1}) + \sigma^2_{X_j}(t_i)}{\tau^2} \qquad (10) \\ &\propto \frac{1}{\tau}. \end{aligned}$$

These formal errors are another convenient way of identifying bad clock estimates since they represent the goodness of fit of the IGS analysis centers' clock estimates. Hence, (10) serves a dual purpose of modelling White FM as well as downweighting bad data in the filter.

E. Outliers and Discrete Steps in Frequency

Outliers are removed by employing a moving window scheme in the following way. The datum $Y^{(j)}(t) = Y^{(j)}_{\mathrm{GPST}}(t)$ (or $Y^{(j)}_{\mathrm{IGST}}(t)$ depending on the iteration) at time step t is removed as an outlier if,

$$\left| Y^{(j)}(t) - \underset{t \epsilon W_{\mathrm{left}} \cup W_{\mathrm{right}}}{\mathrm{median}} \left\{ Y^{(j)}(t) \right\} \right| > 5 \cdot \underset{t \epsilon W_{\mathrm{left}} \cup W_{\mathrm{right}}}{\mathrm{rms}} \left\{ Y^{(j)}(t) \right\},$$

where $W_{\mathrm{left}} = \{t - L \leq t \leq t - l\}$ and $W_{\mathrm{right}} = \{t + l \leq t \leq t + L\}$ with $l < L$. Currently, $l = 30$ minutes and $L = 2$ hours.

Similarly, a discrete step in frequency (e.g. to detect hardware steering changes made at individual IGS stations) for clock j is said to have occured at time step t if,

$$\left| \underset{t \epsilon W_{\mathrm{left}}}{\mathrm{mean}} \left\{ Y^{(j)}(t) \right\} - \underset{t \epsilon W_{\mathrm{right}}}{\mathrm{mean}} \left\{ Y^{(j)}(t) \right\} \right| > 5 \cdot \left(\underset{t \epsilon W_{\mathrm{left}}}{\mathrm{var}} \left\{ Y^{(j)}(t) \right\} + \underset{t \epsilon W_{\mathrm{right}}}{\mathrm{var}} \left\{ Y^{(j)}(t) \right\} \right)^{1/2},$$

In this case, the weight for clock j is set to 0 for 2 hours (and hence is removed from the scale for that duration) and additional noise is injected into the filter for clock j to allow the filter to establish its new rate and drift. Once the new rate and drift are determined, clock j is re-entered into the scale by returning its weight to its nominal value.

In addition to the above outlier detection procedure, particularly poor clocks whose RMS of fractional frequency (using the entire day's data) are larger than 200 nanoseconds/day (e.g. crystal oscillators) are removed from the filter (and hence the scale) altogether for that day.

F. Weighting Scheme

Nominal weights, $\widetilde{w}_j$, for each clock j are calculated daily as the inverse Allan variance measures of that clock. In

the first iteration of the filter, the nominal weights are set as the inverse Allan variance at 3 hours using data referenced to GPST and using only data for the current day being processed. This iteration allows for the detection of unusual (yet slight) changes in the stability of clocks at the various IGS sites which occasionally occur and which are more slight than might be detected by the outlier and frequency step schemes mentioned above. In subsequent iterations, the nominal weights are set to the inverse Allan variance at 6 hours calculated using the current day's data together with data from the previous 6 days. Also, in these subsequent iterations, clocks are referenced to the scale determined from the previous iterations.

In every iteration, nominal weights for each clock are limited to 10% (unless there are fewer than 10 clocks in the ensemble, in which case an upper limit inversely proportional to the number of clocks is chosen). Future enhancements of the package may use a weighting scheme similar to that found in [12] where no absolute upper limit is set, but instead, the upper limit of weight for each clock is *always* chosen inversely proportional to the number of clocks. However, the determination of the proportionality constant is likely to be dependent on the particular mix of clocks in the network and we have decided to allow for more IGS combined clock data before making such a determination.

To ensure the normalization constraint (7) and the upper limit of weights at every epoch as clocks transition in/out of the ensemble, the actual weights, $w_j(t)$, used per epoch and per clock are determined iteratively from the nominal weights $\widetilde{w}_j$. Setting $N = N(t)$ as the number of clocks in the scale at time t, we determine the weights $w_j(t)$ according to the algorithm below. Also, note that as the number $N(t)$ of clocks varies per epoch, we have assumed in the algorithm below that clocks are re-numbered from 1 to $N(t)$ to avoid complicated indexing.

```
U ⟵ max{0.1, 1/N(t)}
for j = 1 to N(t)
   w_j(t) ⟵ w̃_j / Σ_j^{N(t)} w̃_j
end
imposeUL⟵true
while imposeUL
   imposeUL⟵false
   for j = 1 to N(t)
      if w_j(t) > U then
         w_j(t) ⟵ U
         imposeUL⟵true
      end
   end
   sumW⟵ Σ_j^{N(t)} w_j(t)
   for j = 1 to N(t)
      w_j(t) ⟵ w_j(t)/sumW
   end
end
```

One additional problem that may arise in determining the stability (and hence weights) of clocks in the IGS combined clock product is that clocks may appear more stable than is true. This is an artifact of the method in which estimates from each contributing analysis center for each clock are linearly aligned to GPS time in the combination. For example, if a particular clock is used as a reference by *all* of the analysis centers in the reduction of their clock estimates, that clock will appear infinitely stable (i.e. a perfect line) when all of the contributing estimates of that clock are combined and linearly aligned to GPS time. A more insidious case is when several, but not all, analysis centers use the same reference. To guard against these possibilities, the weights for clocks appearing unrealistically stable are automatically forced to zero. Over the six months of IGS combined clock data reduced so far, this situation has not occurred.

G. Steering to GPS Time

In order to utilize the short-term stability of the new IGS time scale while leveraging the longer-term stability of GPS time, the integrated scale is steered to GPS time by applying a two-state (phase and frequency) Linear Quadratic Gaussian (LQG) steering algorithm (cf. [13], [14], and for good references for control and filtering see [15] and [7]). For modularity, this steering filter is implemented separately from that corresponding to (4)-(5). In particular, with input data as $X^{\mathrm{IGST}}_{\mathrm{GPST}}(t)$, the discrete state-space formulation for the steering algorithm is specifed as,

$$\vec{x}(t_{i+1}) = \varphi(\tau)\vec{x}(t_i) + \begin{bmatrix} \tau \\ 1 \end{bmatrix} u(t_i) + \vec{v}(t_i) \quad (11)$$

$$X^{\mathrm{IGST}}_{\mathrm{GPST}}(t) = \mathbf{h}\vec{x}(t) + \xi(t) \quad (12)$$

where $\vec{x}$ is a two-vector representing the phase difference and fractional frequency difference between IGST and GPST, and u is a scalar control corresponding to the fractional frequency change (i.e. steer) being applied. The control u is optimally determined subject to minimizing the quadratic cost functional,

$$J = \sum_i \left(\vec{x}^T(t_i)\mathbf{W_Q}\vec{x}(t_i) + u(t_i)W_R u(t_i) \right), \quad (13)$$

where the matrix $\mathbf{W_Q}$ and scalar W_R are chosen by the designer and determine relative penalties set to the state $\vec{x}$ and control u. For example, if W_R is larger than $\mathbf{W_Q}$, the penalty to steering is large, whereas if $\mathbf{W_Q}$ is larger than W_R, the penalty to steering is small and the system will therefore steer more strongly. A Kalman filter is applied to solve (11)-(12) where one must perform an additional Ricatti equation solve to determine the optimal control u (see [15], [13], and [14] for more details). The exact values of the covariances for $\vec{v}$ and ξ as well as the values for $\mathbf{W_Q}$ and W_R are only relevant with respect to their relative measures as different values of these parameters can produce the same system response. For the values we have chosen, Figure 2 shows the phase and frequency step responses of the system. As the plots in this figure indicate, values were chosen to produce a time-step response of the system of about 10-15 days.

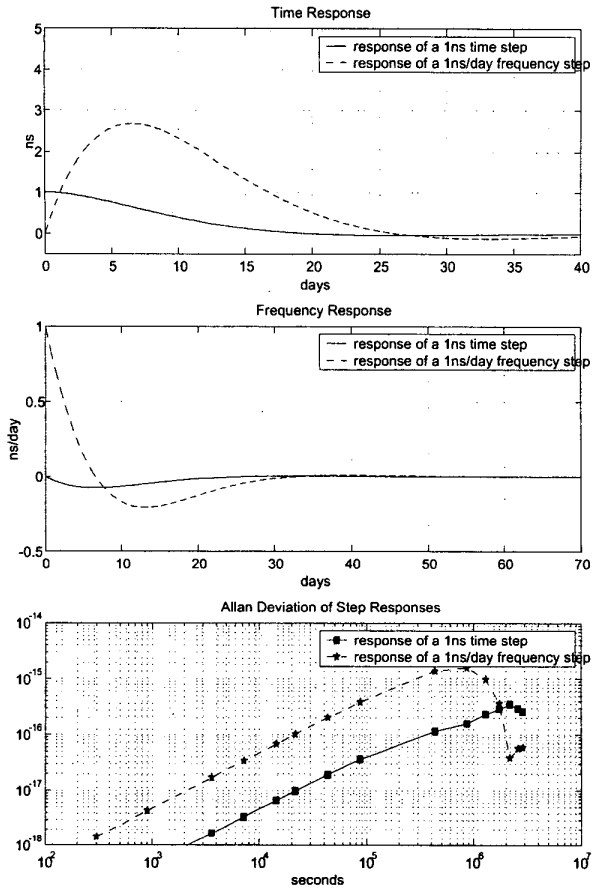

Fig. 2. The impulse time and frequency step responses of the LQG steering algorithm. The top plot shows the time responses of both a 1 nanosecond time step and a 1 nanosecond/day frequency step. The middle plot shows the frequency response of both steps. The bottom plot shows the Allan deviation of the steers applied for each step.

H. A note on the implementation

The application was developed in Matlab and converted to C and/or C++ source code using the new Matlab Compiler, Matlab C/C++ Math Library, and Matlab C++ Graphics Library suites [16]. This suite of packages promotes rapid development of scientific applications—taking advantage of the powerful matrix environment of Matlab (particularly useful in coding filter equations), as well as its efficient I/O routines, which are useful in batch processing of data, and its data visualization routines. Also, the ability to parse out and compile Matlab source code into C/C++ code linked against shared libraries available for many platforms yields efficient compiled code and the ability to port applications independently of the availability of the Matlab program.

III. Results

Though the IGS combined clocks currently consist of approximately 30 hydrogen masers (see TABLE I), many of these are not of sufficient quality to carry significant weight in the new IGS ensemble. Analyzing the results of the ensembling software from the beginning of the IGS combined clock product (November, 2000) through May, 2001 yields a time scale which is largely dominated by 10-15 hydrogen masers. Figures 3, 4, 5, and 6 contain representative results generated by the package depicting various information. In particular, Figure 3 shows a time series of the 15 clocks (referenced to the new steered IGS scale IGST) carrying the largest weight in the ensemble for one week of processing. The legend of the plot contains the weight of each clock in the ensemble for this week as well as the particular quadratic removed from each time series for the purpose of plotting. Figure 5 shows only the time series USNO-IGST of the IGS station located at USNO referenced to the scale, which when compared with Figure 1, provides a quick glance at the improved day-to-day stability of IGST compared against GPST. Figure 4 shows an Allan deviation plot of the 15 highest-weighted clocks (referenced to IGST) for GPS weeks 1091-1092. In particular, the deviation plots show that the stability for IGST is better than 2×10^{-15} at 1 day, which is consistent with results for GPS carrier-phase time transfer found in [17], [18], and [19].

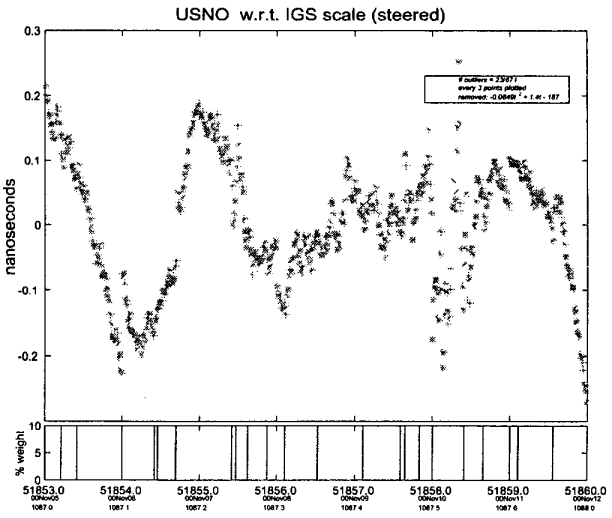

Fig. 5. IGS combined clock estimate of a steered Sigma Tau hydrogen maser located at USNO in Washington, D.C. referenced against the new IGS time scale IGST. Comparison with Figure 1 illustrates the improved time scale stability of IGST over GPST.

Of noteworthy comment is that during the 6 months of data reduced, many of the GPS satellite Block IIR Rubidium clocks often carry slightly more than 1% of the weight in the IGS time scale. Figure 6 shows the Allan deviation for SVN #43 (PRN #13) for such a period.

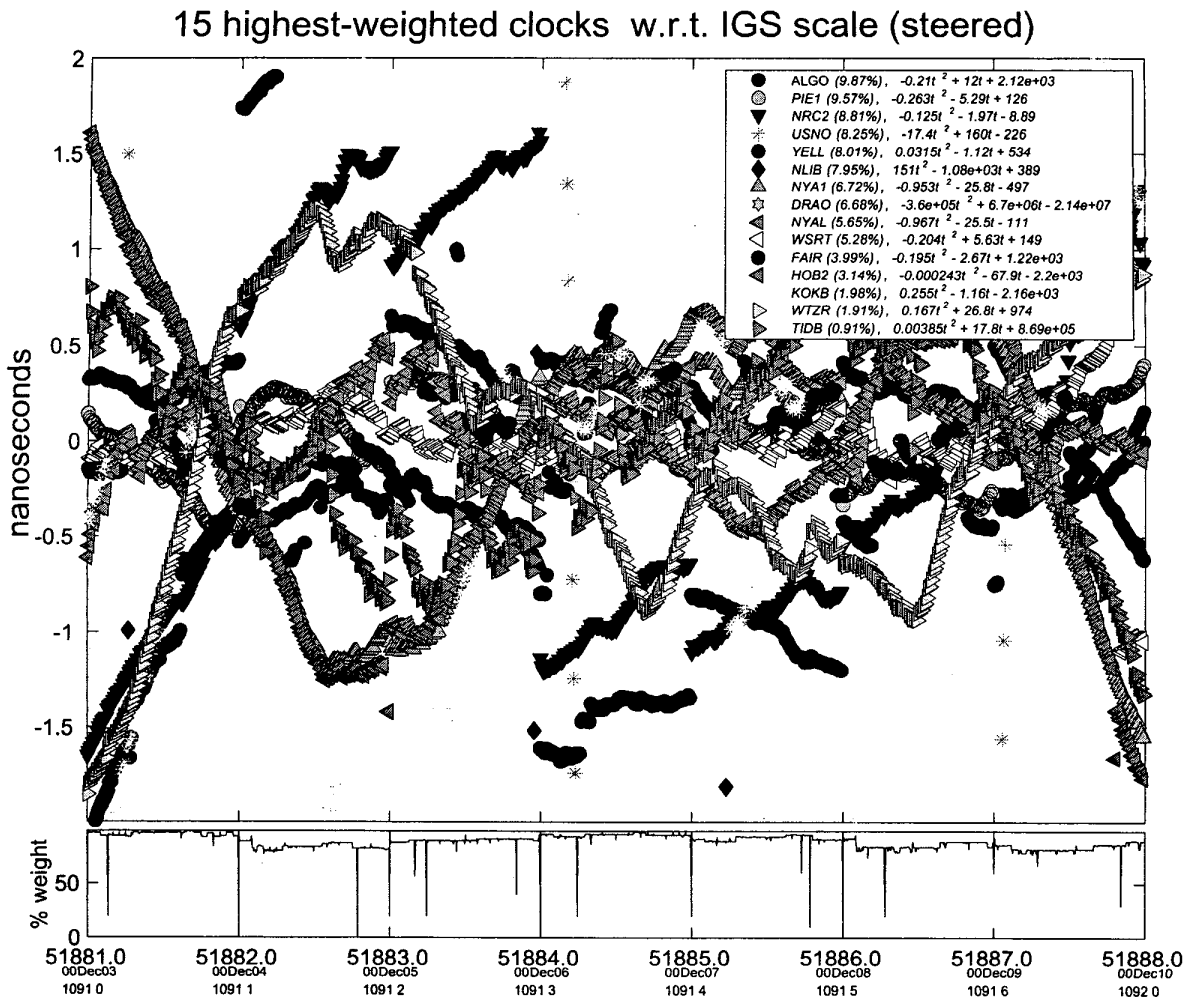

Fig. 3. Phase plot of 15 clocks carrying the highest weight in the IGS time scale IGST in GPS week 1091 (December 3, 2000 - December 9, 2000). Each clock estimate is referenced to IGST and a separate quadratic has been removed from each clock for plotting purposes. The legend of the plot indicates the average weight of each clock in the scale over this period and also the particular quadratic removed (origin used for quadratic removal was t=51881). No other data editing was applied to the clocks in this plot. The smaller bottom plot shows the sum of the per-epoch weights of the 15 clocks. Because this plot was automatically produced in color by the filter package, not every clock will be distinguishable. To obtain a color version with better resolution, contact the authors for a preprint of this paper.

IV. Applications and Future Directions

The use of the new IGS time scale as a completely internal diagnostic tool for characterizing individual site clock behavior will prove a valuable asset as the IGS continues to move toward advancing the use of GPS carrier-phase time/frequency transfer for linking remotely located high-end standards. Other applications include characterizing GPS carrier-phase time transfer and identifying site-dependent effects on time transfer since a time scale with good day-to-day stability which is composed of a globally distributed network of clocks provides a site-independent reference for the site clocks.

As mentioned earlier, relatively few clocks currently dominate the IGS time scale. Therefore, the one effort which is most likely to influence the robustness and quality of the new IGS time scale in the near future is the current clock densification effort being initiated through the IGS/BIPM Pilot Project (see http://maia.usno.navy.mil/gpst.html). The future inclusion into the IGS combined clock product of additional high-quality clocks already in the IGS network, but which are not part of the IGS combined clock product, as well as other quality clocks not yet in the IGS network will no doubt yield improved results.

The new IGS time scale will enter official IGS testing phase in 2001

References

[1] J. Kouba and T. Springer, "New IGS station and satellite clock combination," *GPS Solutions*, vol. 4, no. 4, pp. 31-36, 2001.

[2] J. Zumberge, M. Meflin, M. Watkins, and F. Webb, "Precise

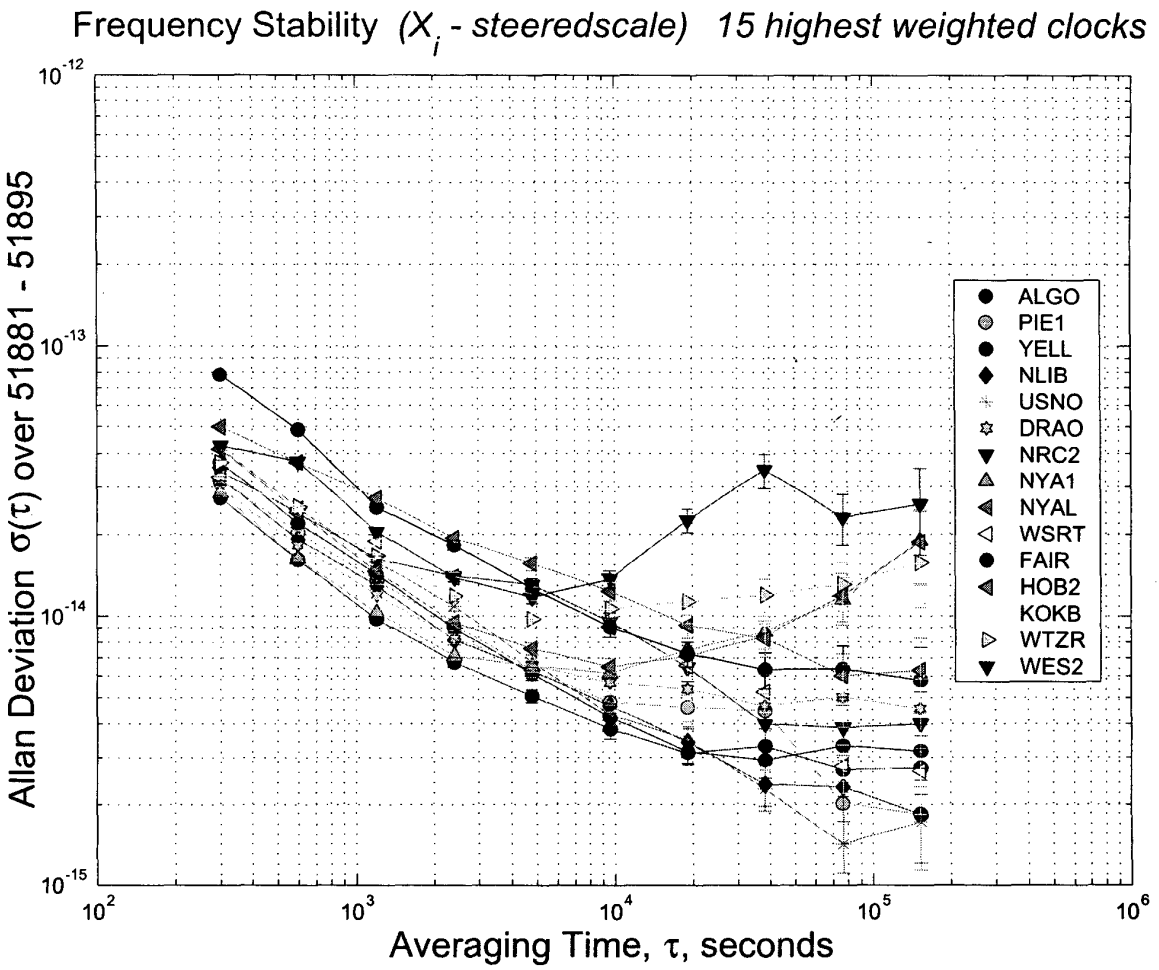

Fig. 4. Allan Deviation plot of the 15 highest-weighted clocks in the IGS time scale IGST for GPS weeks 1091-1092 (December 03, 2000 - December 16, 2000). The clocks are referenced to IGST and no detrending has been performed. Outliers and discrete steps in frequency have been removed from each clock for the generation of this plot. Because this plot was automatically produced in color by the filter package, not every clock will be distinguishable. To obtain a color version with better resolution, contact the authors for a preprint of this paper. The overall banding suggests that the stability of the IGST time scale is better than 2×10^{-15} at 1 day.

point positioning for the efficient and robust analysis of GPS data from large networks," *J. Geophys. Res.*, vol. 102, no. B3, pp. 5005–5017, 1997.

[3] J. Barnes and D. Allan, "Time scale stabilities based on time and frequency kalman filters," *Proc. of the 39th Annual Frequency Control Symposium*, pp. 107–112, May 1985.

[4] D. Percival, "The u.s. naval observatory clock time scales," *IEEE Trans. Instrum. Meas.*, vol. IM-27, no. 4, pp. 376–384, December 1978.

[5] S. Stein, "Advances in time-scale algorithms," *Proc. of the 24th Annual Precise Time and Time Interval (PTTI) Applications and Planning Meeting*, pp. 289–302, December 1992.

[6] L. Breakiron, "private communications," 2001.

[7] R. Brown and P. Hwang, *Introduction to Random Signals and Applied Kalman Filtering*, John Wiley and Sons, New York, 3 edition, 1997.

[8] A. Dierendonck and R. Brown, "Relationship between allan variances and kalman filter parameters," *Proc. of the 16th Annual Precise Time and Time Interval (PTTI) Applications and Planning Meeting*, pp. 273–293, November 1984.

[9] S. Stein and R. Filler, "Kalman filter analysis for real time applications of clocks and oscillators," *Proc. of the 42nd Annual Symposium on Frequency Control*, pp. 447–452, June 1988.

[10] K. Brown., "The theory of the GPS composite clock," *Proc. of ION GPS-91*, pp. 223–241, September 1991.

[11] R. Jones and P. Tryon, "Continuous time series models for unequally spaced data applied to modeling atomic clocks," *SIAM J. Sci. Stat. Comput.*, vol. 8, 1987.

[12] C. Thomas and J. Azoubib, "TAI computation: Study of an alternative choise for implementing an upper limit of clock weights," *Metrologia*, vol. 33, pp. 227–240, 1996.

[13] P. Koppang and R. Leland, "Steering of frequency standards by the use of linear quadratic gaussian control theory," *Proc. of the 27th Annual Precise Time and Time Interval (PTTI) Applications and Planning Meeting*, pp. 257–267, November/December 1987.

[14] D. Matsakis, M. Miranian, and P. Koppang, "Steering strategies for the master clock of USNO," *Proc. of ION GPS 2000*, pp. 933-936, September 2000.

[15] P. Maybeck, *Stochastic Models, Estimation, and Control*, vol. 1-3, Navtech Book and Software Company, Arlington, Virginia, 1994.

[16] "Matlab, matlab compiler, matlab C/C++ math library, and matlab c++ graphics library," *http://www.mathworks.com.*

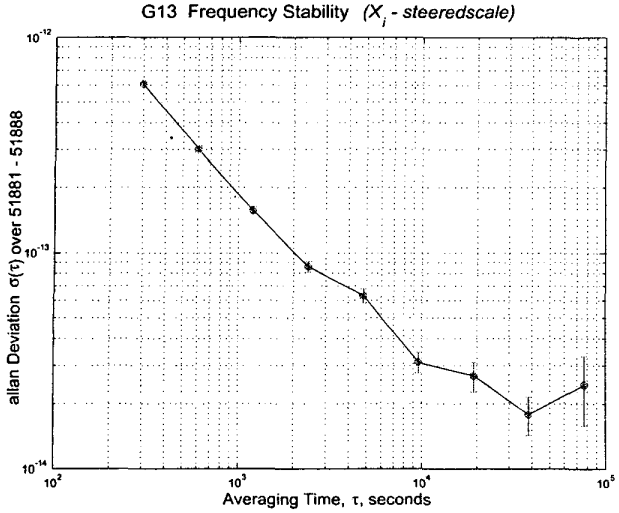

Fig. 6. Allan Deviation plot of SVN 43 (PRN 13) referenced against the IGS time scale IGST for GPS weeks 1091-1092 (December 03, 2000 - December 09, 2000).

[17] L. Young, D. Jefferson, S. Lichten, R. Tjoelker, and L. Maleki, "Formation of a GPS-linked global ensemble of hydrogen masers and comparison to JPL's linear ion trap," *Proc. of the IEEE International Frequency Control Symposium*, pp. 1159–1162, 1996.

[18] K. Larson, J. Levine, L. Nelson, and T. Parker, "Assessment of GPS carrier-phase stability for time-transfer applications," *IEEE Trans. Ultrason., Ferroelect., Freq. Contr.*, vol. 47, no. 2, pp. 484–494, March 2000.

[19] D. Matsakis, K. Senior, and L. Breakiron, "Analysis noise, short-baseline time transfer, and a long-baseline GPS carrier-phase frequency scale," *Proc. of the 31st Annual Precise Time and Time Interval (PTTI) Systems and Applications Meeting*, vol. 34, pp. 491–504, December 1999.